Preliminary Results from the UCLA/SLAC Ultra-High Gradient Cerenkov Wakefield Accelerator Experiment

M. C. Thompson†, H. Badakov, J. B. Rosenzweig, G. Travish*
UCLA Dept. of Physics and Astronomy

M. Hogan, R. Ischebeck, N. Kirby, R. Siemann, D. Walz
Stanford Linear Accelerator Center

P. Muggli – University of Southern California

A. Scott – UCSB Dept. of Physics   R. Yoder - Manhattan College

*Spokesman for the Collaboration at Erice
†Current Affiliation:
Lawrence Livermore National Laboratory

Breakdown Limitations

Researchers such as Kilpatrick, Loew, and Wang have established that the accelerating field achievable in conventional radio frequency accelerators is ultimately limited by the breakdown of the metallic accelerating structure and that the field sustainable in a cavity increases with the frequency of the cavity:

$$E_s = 220(f[\mathrm{GHz}])^{1/3}\ \mathrm{MV/m}$$

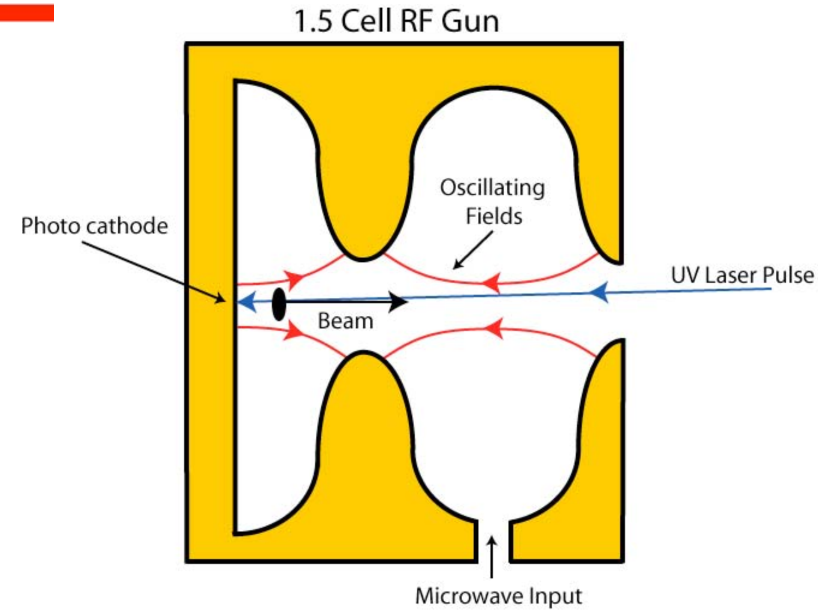

Schematic of a typical S-band RF Photoinjector which is limited by breakdown to an accelerating field on the order of 100 MV/m.

Microwaves

Optical

1 THz, 300 µm

Klystrons

Lasers

X Band:
11.4 GHz, 2.6 cm

Terahertz

Infrared:
28 THz, 10.6 µm

High Frequency Dielectric Accelerators

Dielectric accelerating structures can be driven by many different mechanisms at frequencies from microwave to optical, but electron driven structures operating at THz frequencies have several advantages:

High power THz range operation without external THz source.

Possible breakdown suppression due to relatively low drive beam field photon energies.

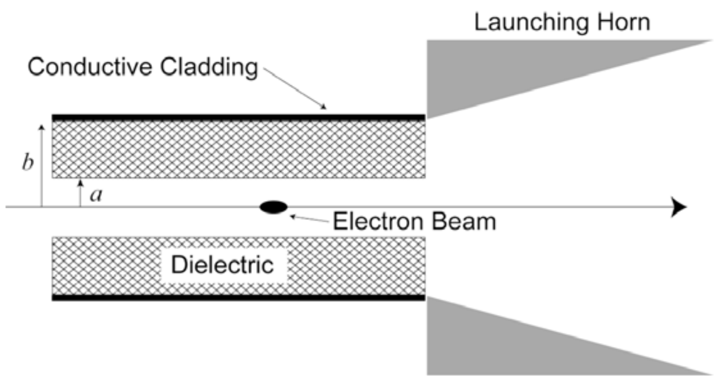

Schematic of a Electron Beam Driven Dielectric Wake Accelerator.

Plasma accelerator class GV/m accelerating fields without the problem of ion collapse.

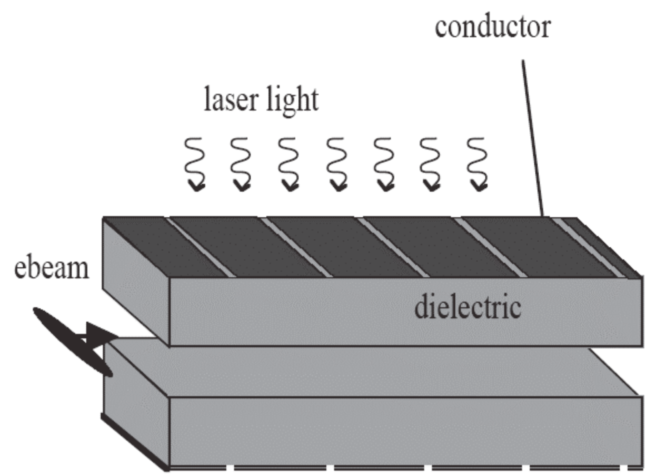

Courtesy R. Yoder

Schematic of a Laser Driven Dielectric Accelerator Structure.

Dielectric Cerenkov Wake Accelerators

The addition of a conductive cladding to a dielectric tube creates a dielectric accelerator structure. When an intense electron beam passes through center of the tube its electric field bends at the Cerenkov angle within the dielectric, reflects off the outside conducting layer, and returns to the axis where it can be used to accelerate other particles.

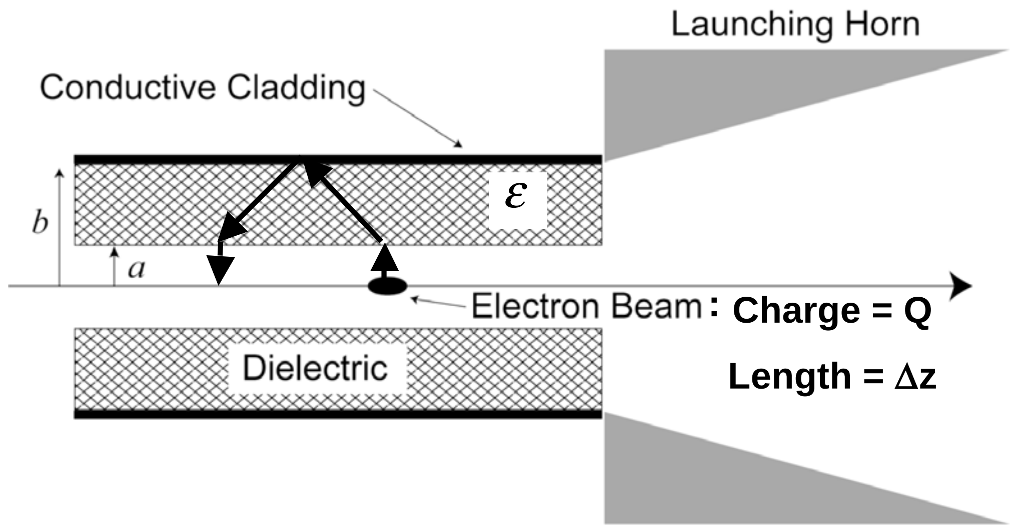

Schematic of the dielectric wake experiment.

On Axis Accelerating Field:

$$E_{z,vac} = \frac{4Q}{a\left[2\frac{\varepsilon}{\sqrt{\varepsilon-1}}\Delta z + a\right]} \xrightarrow[\Delta z << a]{} E_{z,vac} = \frac{2Q}{a^2}$$

Wavelengths of Coherent Cerenkov Radiation Excited:

$$\lambda_n \cong \frac{4(b-a)}{n}\sqrt{\varepsilon - 1}, \quad n = 1,2,3\ldots$$

Ultra-High Gradient Cerenkov Wakefield Accelerator Experimental Plan

The recently achieved 20 μm pulse-length beams obtained at the SLAC Final Focus Test Beam (FFTB) facility made it possible to plan a dielectric wake experiment expected to produce longitudinal fields in excess of 1 GV/m. Previous dielectric wake accelerator research was limited to 10's of MeV/m by the lack of ultra-short drive beams.

Our experiment is designed around the SLAC FFTB beam and dielectric structures made from commercial fused silica capillary tubing.

Table 1: Experiment Design Parameters

Bunch Population (N_b)	1.87 x 10^{10}
Bunch Energy	30 GeV
Beam Radius (σ_r)	10 μm
Beam Length (σ_z)	100 - 20 μm
Inner Dielectric Radius (a)	50 and 100 μm
Outer Dielectric Radius (b)	162 μm
Dielectric Relative Permittivity (ε)	~ 3
Peak Decelerating Field	8 GV/m
Peak Accelerating Field	12 GV/m
Peak Field at Dielectric	22 GV/m

Expected Fundamental Excitation Wavelengths:

350 μm for a = 100 μm (0.9 THz)

633 μm for a = 50 μm (0.5 THz)

OOPIC Simulations for σ_z = 20 μm

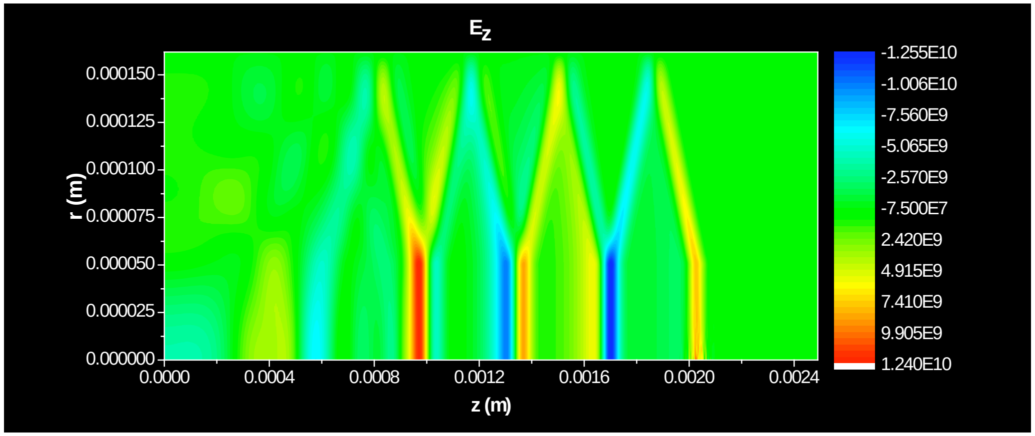

Contour plot showing E_z for a = 50 μm

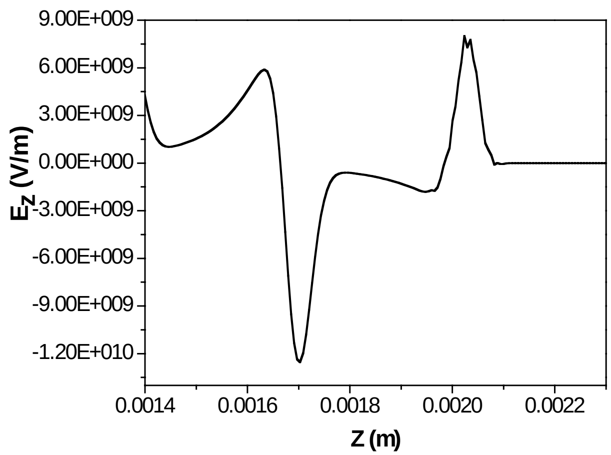

Line out of E_z at
r = 10 μm with a = 50 μm

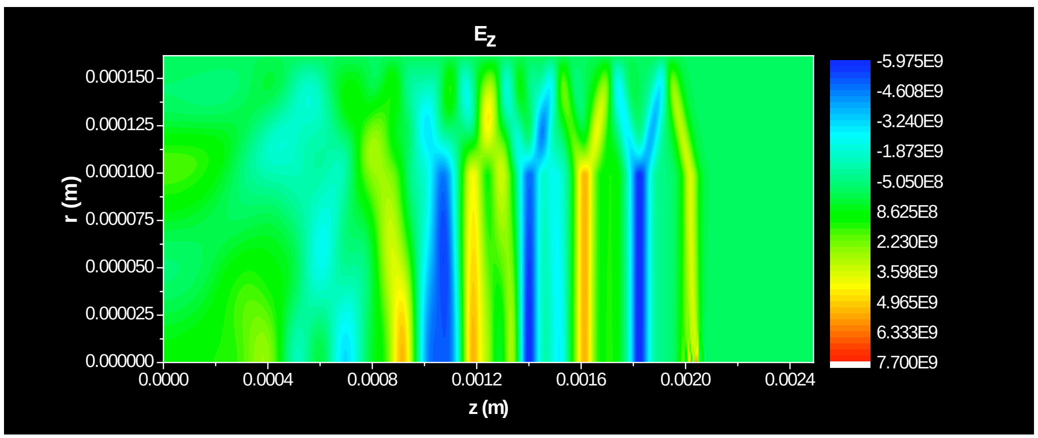

Contour plot showing E_z for a = 100 μm

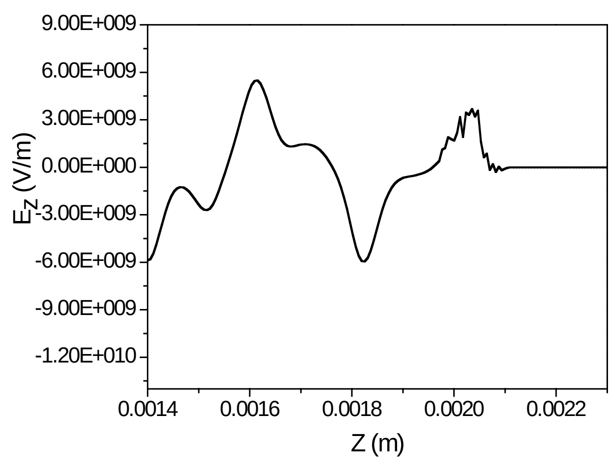

Line out of E_z at
r = 10 μm with a = 100 μm

Experimental Goals and Observables

- Assess Survivability of the Dielectric Material
- Verify the Magnitude and Frequency of the Wakefields

Breakdown:

- When illuminated with a 70 fs laser pulse, the breakdown limit for fused silica is less than 2 GV/m.
- By comparison, our electron beam has σ_t = 67 fs at minimum pulse length and will generate 22 GV/m fields at the inner surface of the a = 50 µm tube.
- Individual photon energies are lower in the wakefield case than the laser case, which may suppress avalanche ionization and perhaps allow higher fields to be tolerated.

Coherent Cerenkov Radiation:

- Using the peak field parameters we find that about 150 mJ of CCR will be produced in the a = 50 µm case and that this energy will be distributed among spectral lines at 633, 316, 211, 158, 126, and 106 µm.
- The THz CCR will have about 5 times the intensity of coherent transition radiation emitted from the surface of the tube end.
- The CCR exiting the end of the dielectric tube will be detected by in vacuum pyroelectric detectors mounted downstream of the tube and slightly off the beam axis.

Realizing the Experiment

Dielectric Tube Samples for this experiment were modified from off the shelf synthetic fused silica capillary tubing ($\varepsilon \approx 3$), which we were able to purchase in 100 and 200 μm ID sizes and coat on the outside with aluminum.

Mounting Blocks are used to hold 10 dielectric tube samples for the experiment. The mounting block are placed on motorized optics mounts and stages so the various samples can be placed onto the beam orbit.

High-Resolution Video Cameras look for optical emissions associated with the breakdown events. We also examine the dielectric tubes after the run to analyze structure damage from breakdown.

Launching Horns, similar to those used in microwave antennas, will boost amount of CCR delivered to the pyroelectric detectors.

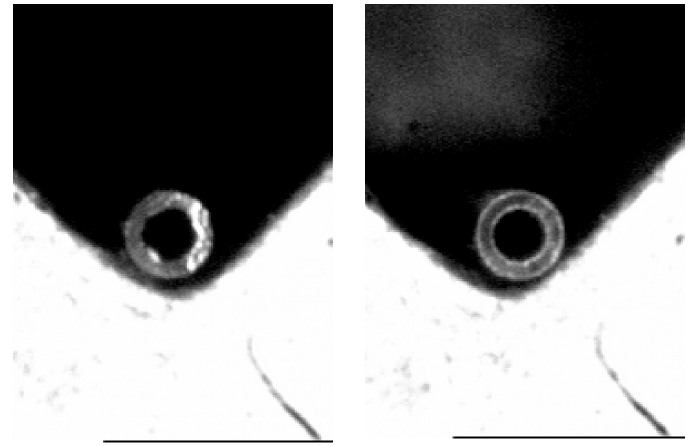

Fiber viewed end on with a microscope. Unpolished at left and polished at right.

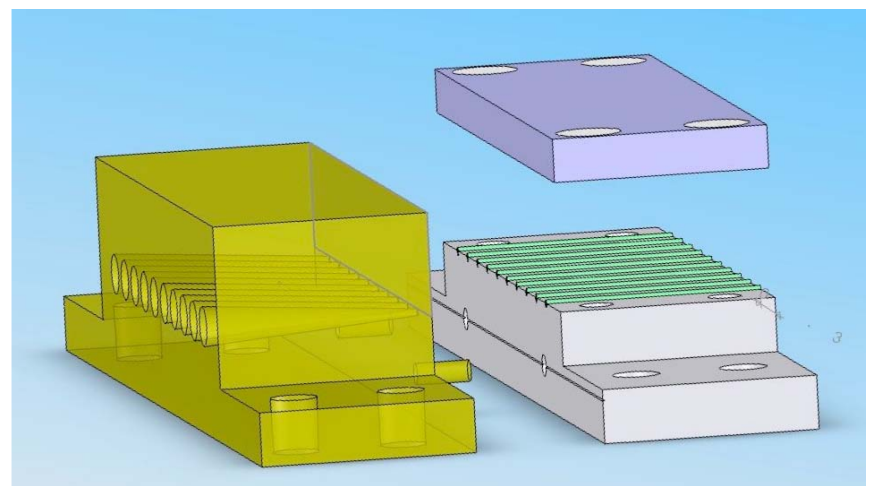

CAD rendering of the capillary tube mounting block with detachable launching horns.

The Equipment

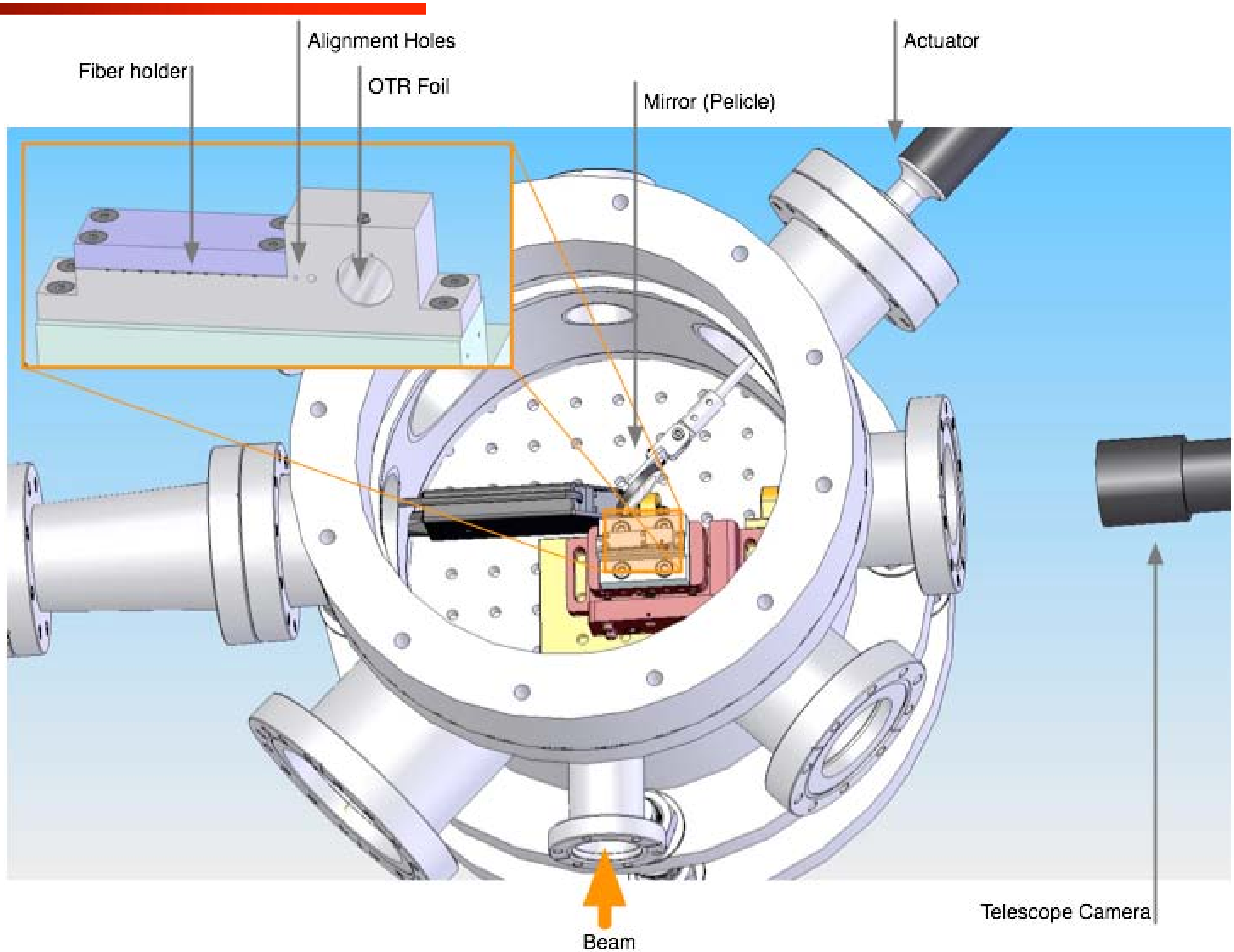

Phase One of the Experiment

The first run of the experiment occurred in Aug 2005. The objective of the run was to examine breakdown thresholds. Direct Measurements of CCR will be attempted in the next run.

Major Observations:

- A sharp increase in visible emission from the capillaries near the mid-range of beam current, probably indicating breakdown.
- Principle form of damage to the dielectric wake structures appear to be vaporization of the aluminum cladding. The fused silica appeared substantially intact.

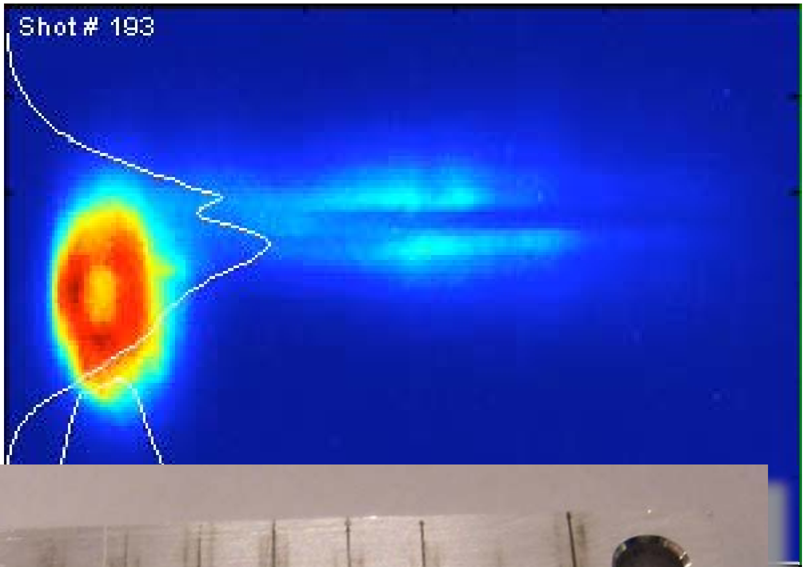

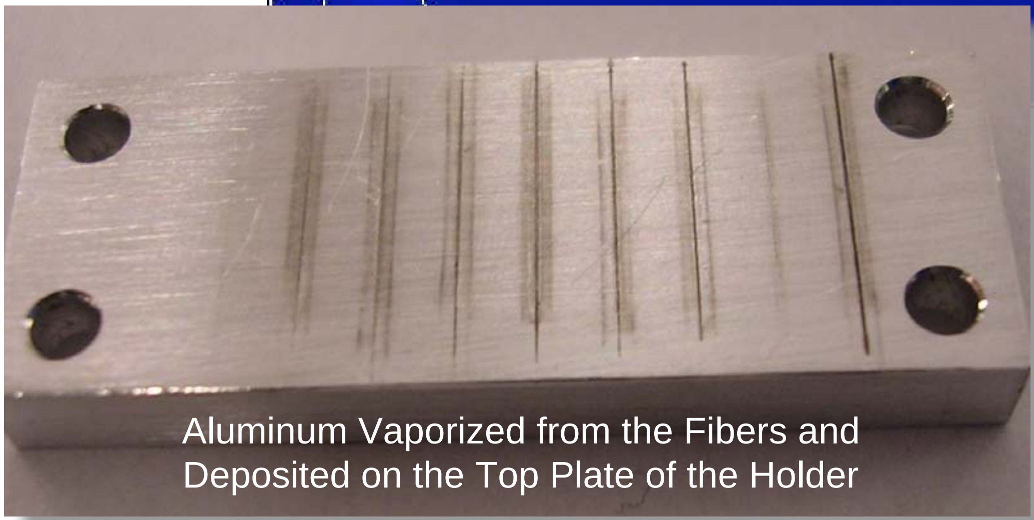
Aluminum Vaporized from the Fibers and Deposited on the Top Plate of the Holder

Breakdown Observations

Most of the observations were of 200 µm ID fibers and the general impression is that the visible light output of the fibers jumped up sharply in the middle of the beam pulse length range. We theorize that the initiation of breakdown discharges are responsible for the increase.

Visible Light Sources Below Threshold:
• Incoherent Cerenkov Radiation, Incoherent Transition Radiation, Scintillation

Visible Light Sources Above Threshold:
• All of the above plus emissions from Plasma formed during breakdown events.

Breakdown fields implied by these preliminary observations should they be confirmed by further analysis:

~ 4 GV/m at the dielectric surface

~ 2 GV/m on axis accelerating field

We are working to quantify these observations.

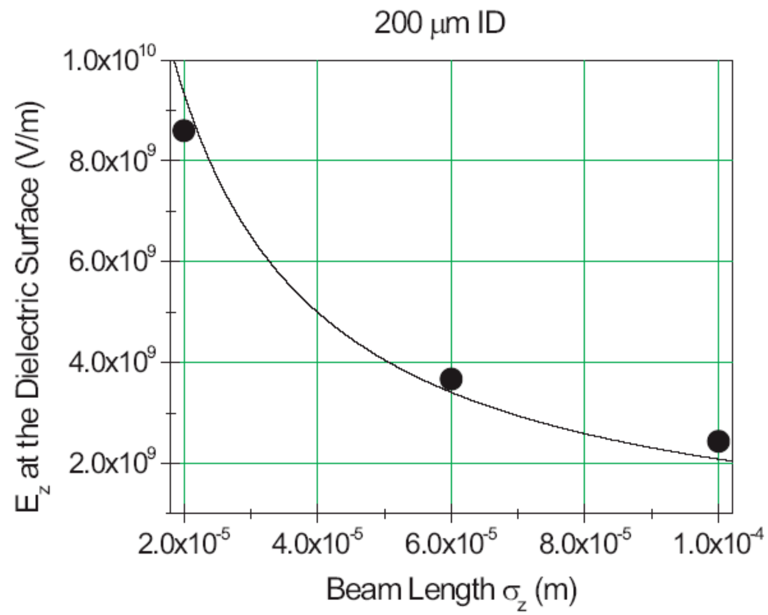

Movie of Fiber Tip

- Frames sorted by increasing peak current.
- Bad (missing) shots removed.
- Visible CCD camera with telescope lens.

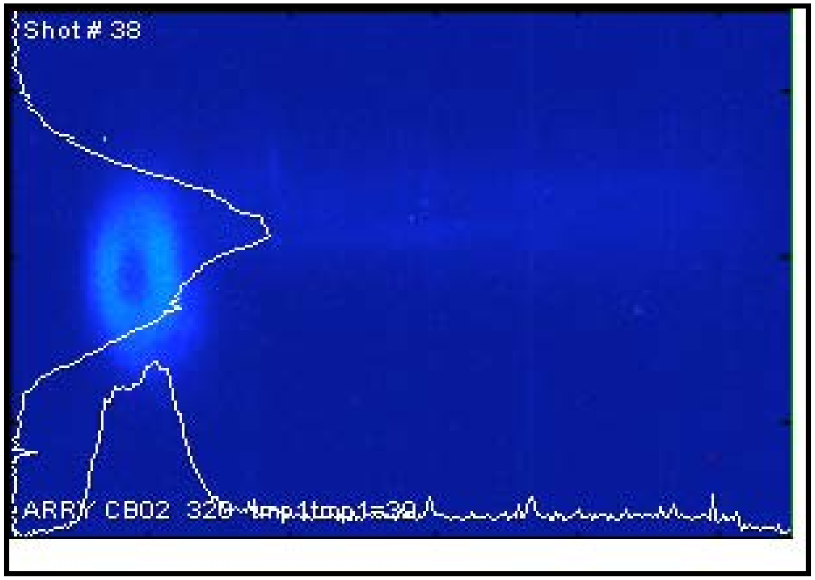

Vaporization of the Aluminum Cladding

Aluminum Vaporized from the Fibers and Deposited on the Top Plate of the Holder

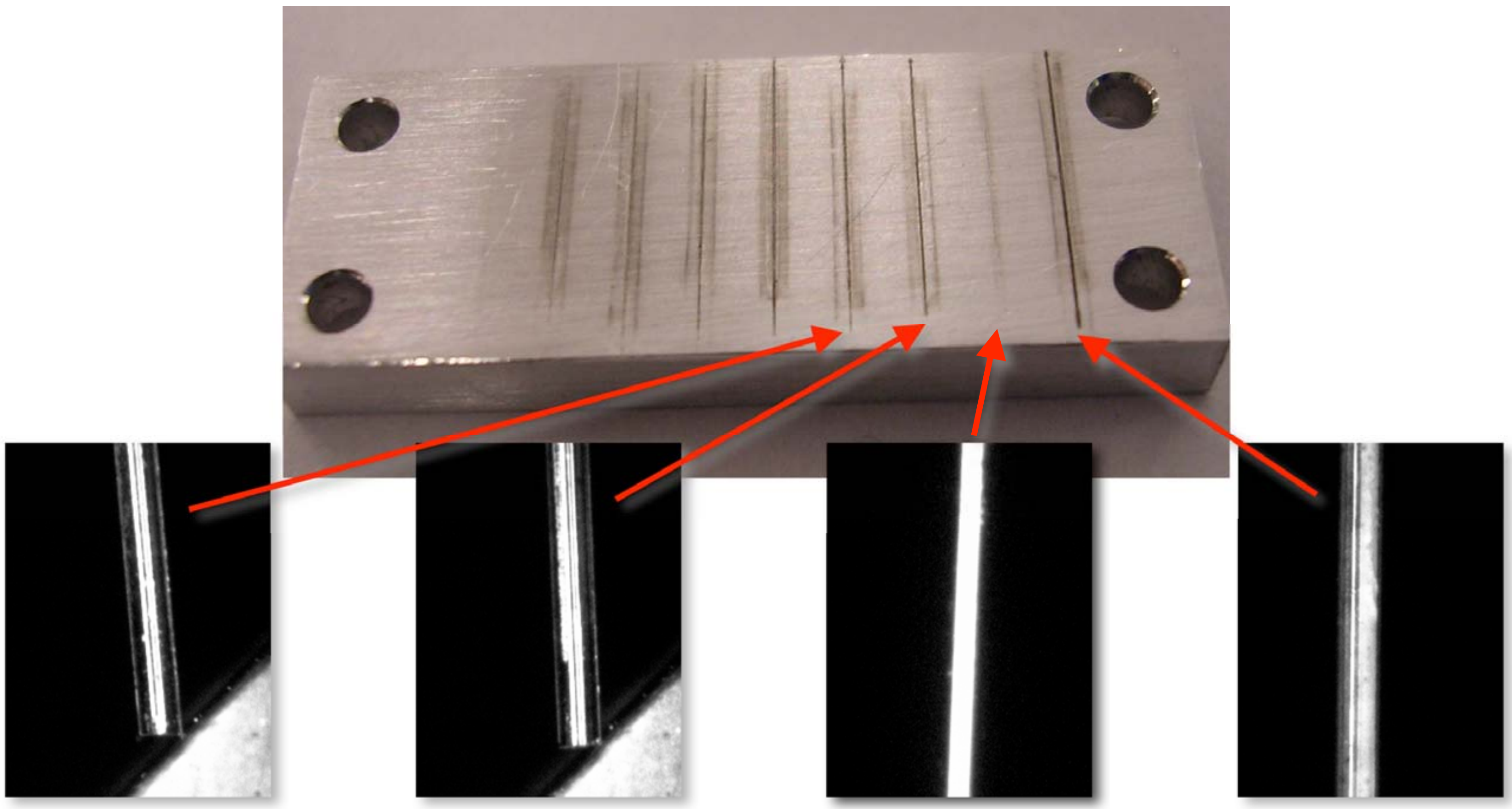

Fiber Exposed to ~50 Shots at Medium Beam Compression – No Visible Aluminum

Fiber Exposed to ~50 Shots Uncompressed Beam – Some Aluminum Remains

Unexposed Fiber ~ 2 μm Aluminum

Fiber Exposed to ~1000 Shots at High Beam Compression – No Visible Aluminum

Pulse Heating Model

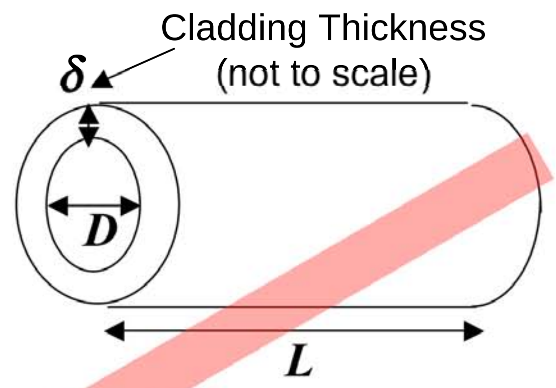

While the evaporation of the aluminum cladding had not been anticipated, a rudimentary model of the resistive heating of the cladding by the image current points to the likely mechanism. Assuming the cladding is thermally isolated, the heating from each beam pulse will add up (and increase the resistance) until the aluminum starts to evaporate.

$$\Delta E_{shot} = R\int I(t)^2\,dt = \frac{c\rho L Q^2}{2\pi^{\frac{3}{2}}\delta D\sigma_z}$$

$$\Delta T = \frac{\Delta E_{shot}}{m_{Al}C_{Al}}$$

$$\rho = \rho_0 + \alpha\Delta T$$

The partial pressure of Aluminum is 8 x 10^{-3} torr (well above the experiment vacuum) at 1200 deg C

Iterating these equation we find that at peak current (Q = 3 nC, σ_z = 20 μm) the cladding reaches 1200 deg C in:

Less then 700 pulses for δ = 2 μm	Less then 50 pulses for δ = 200 nm

Our Cladding thickness is not yet well characterized but lies within this range.

Pulse Heating Model…

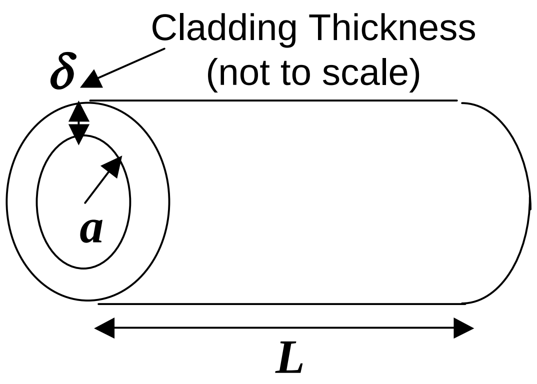

Need to account for frequency dependent skin-depth:

$$\delta_s(\omega) = \sqrt{\frac{2}{\omega\mu_0\sigma_c}}$$

We use the cutoff of the bunch spectrum as the wake frequency. Then, we obtain a skin depth of 53 nm — much less than the cladding layer — for a 65 fs bunch length.

Using the surface resistivity and image current while neglecting wake "bounces", we obtain the energy deposition:

$$\frac{dU}{dA} = -\frac{Q^2}{16\pi^{5/2}a^2\sigma_t^{3/2}}\sqrt{\frac{\mu_0}{\sigma_c}}$$

We obtain ≈32J/m^2 for our parameters (and Q=5 nC).

…Pulse Heating Model…

$$\frac{dU}{dV} = \frac{1}{\delta_s}\frac{dU}{dA} = -\frac{\mu_0 Q^2}{4(2\pi)^{5/2} a^2 \sigma_t^2} = 6.1\times 10^8\, J/m^3$$

Assuming initial thermal dynamics are controlled by electron-electron interactions (short beam transit time)

$$\Delta T = \frac{1}{C_h}\frac{dU}{dM} = \frac{1}{\rho_m C_h}\frac{dU}{dV} \approx 142\ \ J/(kg\cdot {}^\circ K)$$

…multi-pulse heating…
…more work needed

Conclusions

- The prospects for developing GV/m class dielectric accelerators look promising.
- It appears that fused silica holds up well under fields at the GV/m level.
- Resistive heating of the conductive cladding is a significant problem in this extreme environment.

Future Directions

- Further data analysis on all aspects of the experiment should give more insight.
- Clearly the fiber cladding will need to be redesigned with the aim of reducing resistance and increasing thermal coupling.
- The next round of experiments will include measurements of the coherent Cerenkov radiation emitted from the fiber, which will give us more information about the field strengths within the fiber.